

HIERARCHICAL EXPANSION METHOD IN THE SOLUTION OF THE TWO GROUP TWO DIMENSIONAL NEUTRON DIFFUSION EQUATION

Eduardo Lobo Lustosa Cabral
IPEN-CNEN/SP
RAS - Departamento de Reatores
Travessa R, 400 - Cidade Universitária
05508-900 São Paulo, SP

ABSTRACT

A nodal method for the solution of the two-dimensional two-group neutron diffusion equation in rectangular geometry is presented. The method is based on the expansion of the group neutron fluxes by hierarchical functions. The weighted residual procedure is used to obtain the solution equations. The expansion functions are Legendre polynomials adjusted in the rectangular nodes in a novel form, so that corner, side, and area functions are distinguished. The order of the approximation for the side and area expansion functions are up to desired or necessary degree. This formalism has been programmed in a computer code called HEMDC. The two-dimensional IAEA benchmark problem was tested, showing the capability of the method to yield accurate predictions.

Key words: Nodal Methods, Neutron Diffusion, Hierarchical Expansion.

INTRODUCTION

In the last years, nodal methods were developed to obtain accurate, fast answers to the unknown behavior of the neutron flux in nuclear reactor cores, which means the solution of the 2D or 3D space-time transport or diffusion equations, extended over the whole core domain. Although it is possible to simplify the core considering that it is

RESUMO

Este trabalho apresenta um método nodal para a solução da equação de difusão de neutrons em dois grupos e em duas dimensões. O método baseia-se na expansão dos fluxos de neutron, em cada grupo, por funções hierárquicas. O procedimento dos residuos ponderados é utilizado para obter as equações e os coeficientes das funções de expansão. As funções de expansão utilizadas são polinômios de Legendre, ajustados nos nós retangulares de uma maneira inédita, de forma a definir funções de canto, de lado e de área. A ordem das funções de aproximação dos lados e das áreas dos nós é ajustada até o grau necessário ou desejado. Este método foi programado em um programa de computador denominado HEMDC. O problema de referência em duas dimensões da AIEA foi testado e mostrou a capacidade do método em fornecer resultados precisos.

Descritores: Método Nodal, Difusão de Neutrons, Expansão Hierárquica.

composed by a number of large subdomains (nodes) with homogenized neutronic properties, the solution is a quite expensive task, specially in 3D and/or dynamic problems, because of the large number of variables involved.

Nodal methods generally discriminate two levels. The global solution consists in the determination of coupling coefficients (boundary conditions), and the local solution

adjust the flux shape of each node for the coefficients given by the global solution. Techniques for the lower level, such as, polynomial expansions [1, 2], Green's functions [3], response matrices [4], and for the global level, such as, partial currents [1], present interesting features. Partial currents at nodes interfaces usually integrate a set of appropriated coupling coefficients, characterized by a small number of unknowns. Thus, a low iterative effort is required. Success of nodal methods is based on less CPU time and machine memory performance.

In this work a novel method to solve the neutron diffusion equation is presented. The method is based on an expansion of the group neutron fluxes by hierarchical polynomials associated with the weighted-residual classical formulation (Galerkin) [5] to derive the solution equations. The static two group energy equation and a 2D rectangular mesh are used to show the applicability of the method. This method is similar to the nodal methods where a coarse mesh is used but it is a one level method that does not require coupling coefficients at the nodal interfaces.

TWO GROUP NEUTRON DIFFUSION EQUATION AND THE WEIGHTED RESIDUAL METHOD

The static two group neutron diffusion equations are as follows:

$$-D_1 \nabla^2 \phi_1 + \Sigma_1 \phi_1 = \frac{1}{\lambda} (v \Sigma_{11} \phi_1 + v \Sigma_{12} \phi_2) \quad (1)$$

$$-D_2 \nabla^2 \phi_2 + \Sigma_2 \phi_2 = \Sigma_{12} \phi_1 \quad (2)$$

where conventional notations have been used and external neutron sources have not been considered. The boundary conditions can be written in general form as:

$$D_g \bar{\nabla} \phi_g \cdot \bar{n} + b \phi_g = 0 \quad (3)$$

where, the subscript g is either 1 or 2 referring to the fast and to the thermal neutron flux respectively, \bar{n} is the vector normal to the boundary pointing outward to the surface, and b is a constant. Equation (3) allows to

represent the most used boundary conditions. For boundary condition of symmetry plane constant b is zero. For zero net incoming current at the reactor boundary b is equal to 0.5.

To apply the weighted residual method the solution domain, i.e., the reactor is divided in regions, Ω . The regions in this work are rectangles and each region is assumed to be homogeneous, i.e., the properties are constant. The assumption of homogeneous regions is not imposed by the method but it is assumed here for simplicity and in practice this is almost always the case. The fast and thermal neutron fluxes in each region are approximated by a series of functions as follows:

$$\phi_g = \sum_{m=1}^M a_{g,m} P_m(\xi, \eta) \quad (4)$$

where P_m is the m^{th} expansion function, $a_{g,m}$ is a coefficient corresponding to the m^{th} expansion function, M is the number of functions used to approximate the fluxes, and ξ and η are the local coordinates of the region. The expansion functions are special polynomials described in detail in the next section. The local coordinates are related to the x and y coordinates of the global solution domain by the following expressions:

$$\xi = 2 \frac{(x - x_{i,j})}{\Delta x_{i,j}} \quad (5)$$

$$\eta = 2 \frac{(y - y_{i,j})}{\Delta y_{i,j}}$$

where the, $x_{i,j}$ and $y_{i,j}$ are coordinates of the center of domain region i,j , and $\Delta x_{i,j}$ and $\Delta y_{i,j}$ are the region lengths in the x and y directions respectively.

In the weighted residual procedure the coefficients $a_{g,m}$ are the solutions of a set of equations obtained by weighting and integrating of the balance equations over the regions of the domain. The functions used as weight, in the classical Galerkin method and in this work, are the same as the expansion functions. Equations (1) and (2) can be written in general form as follows:

$$-D_g \nabla^2 \phi_g + \Sigma_g \phi_g = F_g \quad (6)$$

where F_g is the fission source for the fast neutron flux and the neutron downscattering for the thermal flux. Applying the weighted residual procedure in equation (6) subject to the boundary conditions given by equation (3), gives the following:

$$\begin{aligned} & - \int_{\Omega} P_m D_g \nabla^2 \phi_g d\Omega + \int_{\Omega} P_m \Sigma_g \phi_g d\Omega + \\ & + \int_{\Gamma} P_m (D_g \vec{\nabla} \phi_g \cdot \vec{n} + b \phi_g) d\Gamma = \int_{\Omega} P_m F_g d\Omega, \\ & \text{for } m=1, \dots, M \end{aligned} \quad (7)$$

where Γ is the boundary of the solution domain. Observe that the third term is presented only for the regions at the reactor boundary. This equation represents a set of M equations for each region. Substituting expression (4) in the above equation results in the following:

$$\begin{aligned} & - \int_{\Omega} D_g P_m \nabla^2 \left(\sum_{n=1}^M a_{g,n} P_n \right) d\Omega + \\ & + \int_{\Omega} P_m \Sigma_g \left(\sum_{n=1}^M a_{g,n} P_n \right) d\Omega + \\ & + \int_{\Gamma} P_m \left[D_g \vec{\nabla} \left(\sum_{n=1}^M a_{g,n} P_n \right) \cdot \vec{n} + \right. \\ & \left. + b \left(\sum_{n=1}^M a_{g,n} P_n \right) \right] d\Gamma = \int_{\Omega} P_m \left(\sum_{n=1}^M f_{g,n} P_n \right) d\Omega, \\ & \text{for } m=1, \dots, M \end{aligned} \quad (8)$$

where $f_{g,n}$ represents the source coefficients. These coefficients are not new unknowns but algebraic combinations of the fast and thermal fluxes coefficients and material properties. Applying the Green's Theorem to the first term and rearranging equation (8), results in the following:

$$\begin{aligned} & D_g^{i,j} \sum_{n=1}^M a_{g,n}^{i,j} \int_{\Omega} (\vec{\nabla} P_m \cdot \vec{\nabla} P_n) d\Omega - \\ & - D_g^{i,j} \sum_{n=1}^M a_{g,n}^{i,j} \int_{\Gamma} (P_m \vec{\nabla} P_n \cdot \vec{n}) d\Gamma + \\ & + \Sigma_g^{i,j} \sum_{n=1}^M a_{g,n}^{i,j} \int_{\Omega} (P_m P_n) d\Omega + \\ & + D_g^{i,j} \sum_{n=1}^M a_{g,n}^{i,j} \int_{\Gamma} (P_m \vec{\nabla} P_n \cdot \vec{n}) d\Gamma + \\ & + b \sum_{n=1}^M a_{g,n}^{i,j} \int_{\Gamma} (P_m P_n) d\Gamma = \\ & = \sum_{n=1}^M f_{g,n}^{i,j} \int_{\Omega} (P_m P_n) d\Omega, \\ & \text{for } m=1, \dots, M \end{aligned} \quad (9)$$

where the superscripts i and j refers to node i, j . In the above equation the second and the fourth terms cancel each other. Now, changing the space coordinates from the global coordinate system, x and y , to the local coordinate system, ξ and η , using equation (5), and rearranging results in the following:

$$\begin{aligned} & D_g^{i,j} \sum_{n=1}^M a_{g,n}^{i,j} \left[\frac{4}{\Delta x_{i,j}^2} \int_{-1}^1 \int_{-1}^1 \left(\frac{\partial P_m}{\partial \xi} \frac{\partial P_n}{\partial \xi} \right) d\xi d\eta + \right. \\ & \left. + \frac{4}{\Delta y_{i,j}^2} \int_{-1}^1 \int_{-1}^1 \left(\frac{\partial P_m}{\partial \eta} \frac{\partial P_n}{\partial \eta} \right) d\xi d\eta \right] + \\ & + \Sigma_g^{i,j} \sum_{n=1}^M a_{g,n}^{i,j} \int_{-1}^1 \int_{-1}^1 (P_m P_n) d\xi d\eta + \\ & + b \sum_{n=1}^M a_{g,n}^{i,j} \left[\int_{-1}^1 [P_m P_n]_{\xi=1} d\eta + \right. \\ & \left. + \int_{-1}^1 [P_m P_n]_{\eta=1} d\xi \right] = \sum_{n=1}^M f_{g,n}^{i,j} \int_{-1}^1 \int_{-1}^1 (P_m P_n) d\xi d\eta, \\ & \text{for } m=1, \dots, M \end{aligned} \quad (10)$$

The last Term of the left hand side is present only for nodes at the reactor boundary. The reactor boundary is represented, as an example in equation (10), located at coordinates $\xi=1$ and $\eta=1$. The above set of equations for each region of the domain can be written in matricial form as follows:

$$\underline{A}_g^{i,j} \underline{a}_g^{i,j} = \bar{f}_g^{i,j} \quad (11)$$

where $\underline{a}_g^{i,j}$ is a $M \times 1$ vector containing the coefficients $a_{g,m}$ for the node i,j , $\bar{f}_g^{i,j}$ is a $M \times 1$ vector formed by the group source of the fast and thermal fluxes for node i,j , and $\underline{A}_g^{i,j}$ is a $M \times M$ nodal matrix, whose element m,n is given by:

$$\begin{aligned} A_{g,m,n}^{i,j} = & 4D_g^{i,j} \left[\frac{1}{\Delta x_{ij}^2} \int_{-1}^1 \int_{-1}^1 \left(\frac{\partial P_m}{\partial \xi} \frac{\partial P_n}{\partial \xi} \right) d\xi d\eta + \right. \\ & \left. + \frac{1}{\Delta y_{ij}^2} \int_{-1}^1 \int_{-1}^1 \left(\frac{\partial P_m}{\partial \eta} \frac{\partial P_n}{\partial \eta} \right) d\xi d\eta \right] + \\ & + \sum_g^{i,j} \int_{-1}^1 \int_{-1}^1 (P_m P_n) d\xi d\eta + b \int_{-1}^1 [P_m P_n]_{\xi=1} d\eta + \\ & + b \int_{-1}^1 [P_m P_n]_{\eta=1} d\xi \end{aligned} \quad (12)$$

The m^{th} component of the source vector $\bar{f}_g^{i,j}$ for node i,j for the fast flux is given by:

$$\begin{aligned} f_{1,m}^{i,j} = & \frac{1}{\lambda} \left[v_1 \sum_{n=1}^M \left(a_{1,n}^{i,j} \int_{-1}^1 \int_{-1}^1 P_m P_n d\xi d\eta \right) + \right. \\ & \left. + v_2 \sum_{n=1}^M \left(a_{2,n}^{i,j} \int_{-1}^1 \int_{-1}^1 P_m P_n d\xi d\eta \right) \right] \end{aligned} \quad (13)$$

and, for the thermal flux by,

$$f_{2,m}^{i,j} = \sum_{n=1}^M \left(a_{1,n}^{i,j} \int_{-1}^1 \int_{-1}^1 P_m P_n d\xi d\eta \right) \quad (14)$$

Equation (11) represents the neutron balance equation for energy group g for a single node. However, more than one node share the same coefficients $a_{g,m}$, as the next sections explain.

HIERARCHICAL FUNCTIONS

In finite element method the coefficients $a_{g,m}$ are identified with the fluxes

at specified locations. This identification has been widely followed in the finite element literature and has the merit of assigning a "physical" meaning to the parameters $a_{g,m}$. There is, however, a disadvantage in this definition. This is apparent if the shape functions for linear, quadratic, and cubic polynomials, for one dimensional case, and the resulting nodal matrices are examined.

Figure (1) shows a typical two node linear element, the two nodes are numbered as node 0 and node 1.

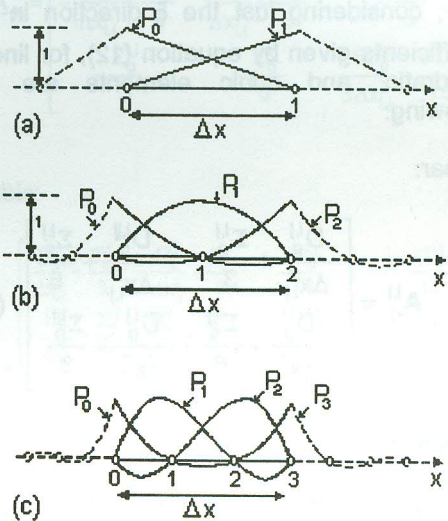


Figure 1: One-dimensional elements and associated standard shape functions of (a) linear, (b) quadratic, and (c) cubic form (from [5]).

With the nodes equally spaced within the node, the shape functions are normally the following:

Linear:

$$P_0 = -\frac{\xi-1}{2}, \quad P_1 = \frac{\xi+1}{2} \quad (15)$$

Quadratic:

$$\begin{aligned} P_0 &= -\frac{\xi(\xi-1)}{2}, & P_1 &= -(\xi-1)(\xi+1), \\ P_2 &= \frac{\xi(\xi+1)}{2} \end{aligned} \quad (16)$$

Cubic:

$$\begin{aligned}
 P_0 &= -\frac{9}{16} \left(\xi + \frac{1}{3}\right) \left(\xi - \frac{1}{3}\right) (\xi - 1); \\
 P_1 &= \frac{27}{16} (\xi + 1) \left(\xi - \frac{1}{3}\right) (\xi - 1); \\
 P_2 &= -\frac{27}{16} (\xi + 1) \left(\xi + \frac{1}{3}\right) (\xi - 1); \\
 P_3 &= \frac{9}{16} (\xi + 1) \left(\xi + \frac{1}{3}\right) \left(\xi - \frac{1}{3}\right) \quad (17)
 \end{aligned}$$

For these functions the nodal matrix $A_g^{i,j}$, considering just the ξ direction in the coefficients given by equation (12), for linear, quadratic, and cubic elements are the following:

Linear:

$$A_g^{i,j} = \begin{bmatrix} \frac{D_g^{i,j}}{\Delta x_{i,j}^2} + \frac{\Sigma_g^{i,j}}{3} & -\frac{D_g^{i,j}}{\Delta x_{i,j}^2} + \frac{\Sigma_g^{i,j}}{6} \\ -\frac{D_g^{i,j}}{\Delta x_{i,j}^2} + \frac{\Sigma_g^{i,j}}{6} & \frac{D_g^{i,j}}{\Delta x_{i,j}^2} + \frac{\Sigma_g^{i,j}}{3} \end{bmatrix} \quad (18)$$

Quadratic:

$$A_g^{i,j} = \begin{bmatrix} \frac{7D_g^{i,j}}{3\Delta x_{i,j}^2} + \frac{2\Sigma_g^{i,j}}{15} & -\frac{8D_g^{i,j}}{3\Delta x_{i,j}^2} + \frac{\Sigma_g^{i,j}}{15} & \frac{D_g^{i,j}}{3\Delta x_{i,j}^2} - \frac{\Sigma_g^{i,j}}{30} \\ -\frac{8D_g^{i,j}}{3\Delta x_{i,j}^2} + \frac{\Sigma_g^{i,j}}{15} & \frac{16D_g^{i,j}}{3\Delta x_{i,j}^2} + \frac{8\Sigma_g^{i,j}}{15} & -\frac{8D_g^{i,j}}{3\Delta x_{i,j}^2} + \frac{\Sigma_g^{i,j}}{15} \\ \frac{D_g^{i,j}}{3\Delta x_{i,j}^2} - \frac{\Sigma_g^{i,j}}{30} & -\frac{8D_g^{i,j}}{3\Delta x_{i,j}^2} + \frac{\Sigma_g^{i,j}}{15} & \frac{7D_g^{i,j}}{3\Delta x_{i,j}^2} + \frac{2\Sigma_g^{i,j}}{15} \end{bmatrix} \quad (19)$$

Cubic:

$$A_g^{i,j} = \begin{bmatrix} \frac{37D_g^{i,j}}{40\Delta x_{i,j}^2} + \frac{8\Sigma_g^{i,j}}{105} & \frac{189D_g^{i,j}}{40\Delta x_{i,j}^2} + \frac{33\Sigma_g^{i,j}}{560} & \frac{27D_g^{i,j}}{20\Delta x_{i,j}^2} + \frac{3\Sigma_g^{i,j}}{140} & \frac{13D_g^{i,j}}{40\Delta x_{i,j}^2} + \frac{19\Sigma_g^{i,j}}{1680} \\ \frac{189D_g^{i,j}}{40\Delta x_{i,j}^2} + \frac{33\Sigma_g^{i,j}}{560} & \frac{54D_g^{i,j}}{40\Delta x_{i,j}^2} + \frac{27\Sigma_g^{i,j}}{70} & \frac{297D_g^{i,j}}{40\Delta x_{i,j}^2} + \frac{27\Sigma_g^{i,j}}{560} & \frac{27D_g^{i,j}}{20\Delta x_{i,j}^2} + \frac{3\Sigma_g^{i,j}}{140} \\ \frac{27D_g^{i,j}}{20\Delta x_{i,j}^2} + \frac{3\Sigma_g^{i,j}}{140} & \frac{297D_g^{i,j}}{40\Delta x_{i,j}^2} + \frac{27\Sigma_g^{i,j}}{560} & \frac{54D_g^{i,j}}{40\Delta x_{i,j}^2} + \frac{70\Sigma_g^{i,j}}{560} & \frac{189D_g^{i,j}}{40\Delta x_{i,j}^2} + \frac{33\Sigma_g^{i,j}}{560} \\ \frac{13D_g^{i,j}}{40\Delta x_{i,j}^2} + \frac{19\Sigma_g^{i,j}}{1680} & \frac{27D_g^{i,j}}{20\Delta x_{i,j}^2} + \frac{3\Sigma_g^{i,j}}{140} & \frac{189D_g^{i,j}}{40\Delta x_{i,j}^2} + \frac{33\Sigma_g^{i,j}}{560} & \frac{37D_g^{i,j}}{40\Delta x_{i,j}^2} + \frac{8\Sigma_g^{i,j}}{105} \end{bmatrix} \quad (20)$$

As the nodal matrix in the above equations for each order of approximation are completely different, each level of approximation results

in a completely new nodal matrix, and thus the equation set has to be entirely reevaluated if it is decided to resolve a problem using shape functions of a higher degree. This type of approximation contrast sharply with the continuous function approximation given by equation (4), in which when the solution is refined by increasing the total number M of the expansion functions used, the form of the lower order expansion functions remained unaltered. In this approach the expansion functions represent simply additive refinements of higher order. Such expansion functions are called hierarchical, as their contribution to the approximation will be of diminish importance as the order increase.

Further, if the chosen expansion functions are orthogonal, the nodal matrices obtained at each stage of refinement ensure a better conditioning of the system equation to be solved and show a diagonal structure. Although completely diagonality of the approximation is almost impossible to achieve, it must be attempted to achieve as weak a coupling as possible between the various levels of approximation. This has the numerical advantage that; (1) the convergence of the solution is faster; and, (2) because a certain loss of accuracy always occurs in the computation of large problems due to numerical roundoff, the successive coefficients $a_{g,m}$, decreasing in importance, can then tolerate a larger amount of numerical inaccuracy without seriously affecting the quality of the total solution.

As mentioned previously, an optimal form of the hierarchical functions is one that results in a diagonal equation system. In the problem of neutron diffusion the predominant term in the nodal matrix is the diffusion terms which possesses the following general form:

$$D_g \int_{\Omega} \frac{\partial P_m}{\partial \xi} \frac{\partial P_n}{\partial \xi} d\Omega \quad (21)$$

If expansion function sets containing the appropriate polynomials can be found for which such integrals are zero for $m \neq n$, then orthogonality is achieved and the coupling between successive solution disappears.

Clearly, the linear expansion over a one dimensional element can only be given by the shape function of equation (15) and cannot be improved upon. However,

hierarchical format can be achieved over this element if higher order polynomials are used to modify this linear expansion. One set of polynomial functions which posses this orthogonality property over the range $-1 \leq \xi \leq 1$ is the set of Legendre polynomials $P_m(\xi)$. The Legendre polynomial of degree m is given by the following recurrence formula [5]:

$$P_m = \frac{1}{(m-1)!} \frac{1}{2^{m-1}} \frac{d^m}{d\xi^m} [(\xi^2 - 1)^m] \quad (22)$$

Integrating this polynomial for $m=2,3,4,5$ in turn gives,

$$P_2 = \xi^2 - 1, \quad P_4 = \frac{1}{4}(15\xi^4 - 18\xi^2 + 3)$$

$$P_3 = 2(\xi^3 - \xi), \quad P_5 = 7\xi^5 - 10\xi^3 + 3\xi \quad (23)$$

A plot of these functions, up to the third degree, is given in figure (2).

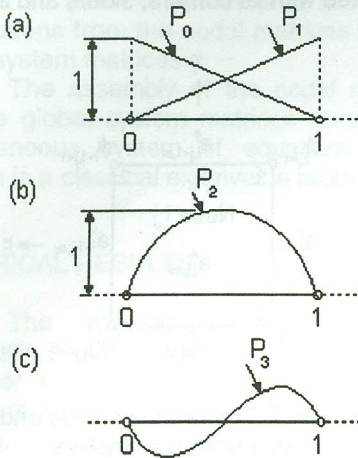


Figure 2: Hierarchical element shape functions of nearly orthogonal form, (a) linear, (b) quadratic, and (c) cubic.

For these polynomials the nodal matrix $\underline{A}_g^{i,j}$, considering just the ξ direction in the coefficients given by equation (12), for linear, quadratic, and cubic elements are the following:

Linear:

$$\underline{A}_g^{i,j} = \begin{bmatrix} D_g^{i,j} + \frac{\Sigma_g^{i,j}}{3} & -\frac{D_g^{i,j}}{\Delta x_{i,j}^2} + \frac{\Sigma_g^{i,j}}{6} \\ -\frac{D_g^{i,j}}{\Delta x_{i,j}^2} + \frac{\Sigma_g^{i,j}}{6} & D_g^{i,j} + \frac{\Sigma_g^{i,j}}{3} \end{bmatrix} \quad (24)$$

Quadratic:

$$\underline{A}_g^{i,j} = \begin{bmatrix} D_g^{i,j} + \frac{\Sigma_g^{i,j}}{3} & -\frac{D_g^{i,j}}{\Delta x_{i,j}^2} + \frac{\Sigma_g^{i,j}}{6} & -\frac{\Sigma_g^{i,j}}{3} \\ -\frac{D_g^{i,j}}{\Delta x_{i,j}^2} + \frac{\Sigma_g^{i,j}}{6} & D_g^{i,j} + \frac{\Sigma_g^{i,j}}{3} & -\frac{\Sigma_g^{i,j}}{3} \\ -\frac{\Sigma_g^{i,j}}{3} & -\frac{\Sigma_g^{i,j}}{3} & \frac{16D_g^{i,j}}{3\Delta x_{i,j}^2} + \frac{8\Sigma_g^{i,j}}{15} \end{bmatrix} \quad (25)$$

Cubic:

$$\underline{A}_g^{i,j} = \begin{bmatrix} D_g^{i,j} + \frac{\Sigma_g^{i,j}}{3} & -\frac{D_g^{i,j}}{\Delta x_{i,j}^2} + \frac{\Sigma_g^{i,j}}{6} & -\frac{\Sigma_g^{i,j}}{3} & \frac{2\Sigma_g^{i,j}}{15} \\ -\frac{D_g^{i,j}}{\Delta x_{i,j}^2} + \frac{\Sigma_g^{i,j}}{6} & D_g^{i,j} + \frac{\Sigma_g^{i,j}}{3} & -\frac{\Sigma_g^{i,j}}{3} & -\frac{2\Sigma_g^{i,j}}{15} \\ -\frac{\Sigma_g^{i,j}}{3} & -\frac{\Sigma_g^{i,j}}{3} & \frac{16D_g^{i,j}}{3\Delta x_{i,j}^2} + \frac{8\Sigma_g^{i,j}}{15} & 0 \\ \frac{2\Sigma_g^{i,j}}{15} & -\frac{2\Sigma_g^{i,j}}{15} & 0 & \frac{164D_g^{i,j}}{5\Delta x_{i,j}^2} + \frac{32\Sigma_g^{i,j}}{105} \end{bmatrix} \quad (26)$$

In each step above it can be seen that, as the approximation is refined, the matrices produced by the previous stage of approximation reoccur and need not be recomputed.

Obviously absolute orthogonality is not achieved but it is easily observed that the terms of the main diagonal are predominant over the other terms.

TWO DIMENSIONAL RECTANGULAR HIERARCHICAL SHAPE FUNCTIONS

With the one-dimensional hierarchical expansion functions already established, the generation of hierarchical expansion functions for rectangular two-dimensional elements is trivial. The identification (or connection) of hierarchical variables associated with any element side with the same value on the adjacent element will automatically guarantee

the uniqueness of the approximation of the neutron fluxes along that side, and continuity of the fluxes will be ensured. Any product of a one-dimensional hierarchical shape function in the local element variable along a side, say ξ , with a linear (or hierarchical) function in the other local element direction, η , proves to be acceptable, and polynomial terms (of any degree) can be obtained by forming such simple products. Using the one-dimensional functions of equation (23), the expansion functions for the element shown in figure 3 can be written as follows.

Typical corner node (3):

$$P_3(\xi, \eta) = \frac{1}{4}(1 + \eta\xi)(1 - \xi) \quad (27)$$

Typical side (2-3):

$$P_{2(2-3)}(\xi, \eta) = \frac{1}{2}(1 + \eta)(\xi^2 - 1) \quad (28)$$

$$P_{3(2-3)}(\xi, \eta) = \frac{1}{6}(1 + \eta)(\xi^3 - \xi) \quad (29)$$

Observe that the value of these functions is zero in the two corners 2 and 3, and in the other three sides.

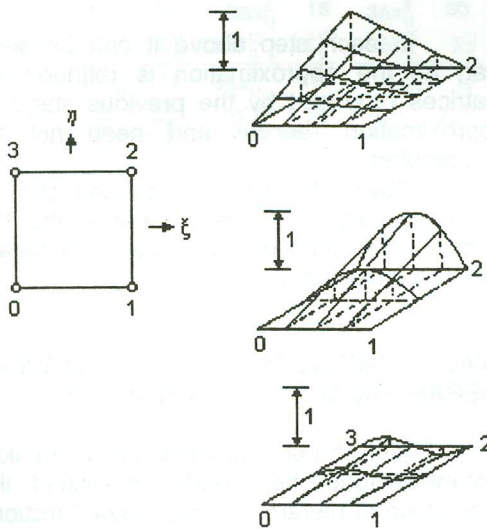


Figure 3: Hierarchical element expansion functions on a rectangular node.

Expansion functions to improve the solution in a single node can be obtained by the product of two functions of degree greater than two in the both directions. For instance,

$$P_{2(\text{area})}(\xi, \eta) = \frac{1}{4}(\xi^2 - 1)(\eta^2 - 1) \quad (30)$$

provides a suitable expansion function which will be associated with a parameter that is not connected between nodes, i.e., a parameter that is internal to a single node. This parameter can be thought as representing the nodal area. Observe that the value of this function is zero in the four corners and in the four sides of the node.

The numbering of nodal and hierarchical parameters in a logical sequence presents interesting problems as the label corresponding to a hierarchical degree of freedom can be associated either with an element side or with a single element. Figure 4 shows a node with the parameters associated with its corners, sides, and area.

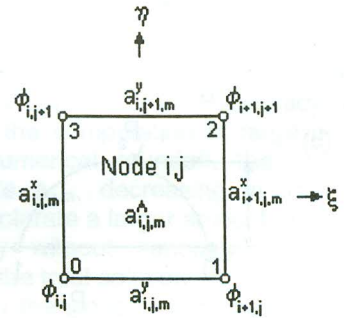


Figure 4: 2D rectangular node and its associated parameters.

In figure 4, $\phi_{i,j}$ are the corner parameters associated with the linear expansion functions, $a^x_{i,j,m}$ and $a^y_{i,j,m}$ are the side parameters associated with the side expansion functions, and $a^A_{i,j,m}$ are the area parameters associated with the area expansion functions. The order of the approximation for the side and area expansion functions are up to desired or necessary degree.

In passing it should be observed that it is very easy to add polynomial expansions locally to achieve a refinement in the region where the neutron fluxes varies most rapidly

and where the approximation is therefore prone to the largest errors.

Observe that the corner parameters are physically associated with the group flux at the corner points. The parameter $\phi_{i,j}$ is associated with expansion function P_0 in node i,j . Also, this same parameter is associated with function P_1 in node $i,j-1$, with function P_2 in node $i-1,j-1$, and with function P_3 in node $i-1,j$. Therefore, the corner parameters are connected to four different nodes through four different expansion functions. The side parameters $a_{i,j,m}^x$ and $a_{i,j,m}^y$ are connected to two nodes and they do not have a physical meaning as the corner parameters. The area parameters are connected to a single node only.

As mentioned, equation (11) represents the neutron balance for energy group g for a single node, and as observed the corner and side parameters are shared by more than a single node. Therefore, before these coefficients can be calculated, there must be an assembly process to add up the contributions from the nodal matrices into the global system matrices.

The assembly of the nodal matrices into the global system matrices results in a homogeneous system of equations whose solution is a classical eigenvalue problem.

NUMERICAL RESULTS

The method presented in the previously sections were implemented in a computer code denominated HEMDC. The procedure used to calculate the coefficients $a_{g,m}$, i.e., the neutron fluxes, is the normally used in neutronic codes. The process consists of an internal and an external iteration. In the internal iteration the source is fixed and the Gauss-Siedel relaxation method is used to solve the system of equations. The outer iteration step is used to update the source given the new solution obtained from the inner iteration step. The method of Chebyshev Polynomials applied to the coefficients $a_{g,m}$ is used to accelerate the convergence of the solution. For the results presented in this work one inner iteration is used for each outer iteration.

In the present work the 2D International Atomic Energy Agency (IAEA) Benchmark Problem have been calculated

and related to other results reported. This problem is a 2D simplified four-zone LWR, consisting in 177 20 cm X 20 cm fuel assemblies, and reflected radially and axially by 20 cm of water [6].

Results from the code HEMDC of three solutions for an octant with square mesh of 20 cm and 10 cm are given. For the 20 cm mesh 3rd and 5th order polynomial expansion are used. For the 10 cm mesh only a 3rd order expansion is performed.

Table 1 presents the k-effective for the three solutions together with results from other codes, obtained from [6].

Table 1: Results of k-effective from several codes and conditions

Code	(mesh size, order)	K-effective
HEMDC	20 cm, 3 rd	1.029606
HEMDC	20 cm, 5 th	1.029553
HEMDC	10 cm, 3 rd	1.029582
MEDIUM-2 [7]	3 1/3 cm	1.029585
MEDIUM-2 [7]	10 cm	1.029611
FEMB [8]	4.7 cm, 2 nd	1.0296
FERM [4]	-	1.02961
RHENO [9]	-	1.029565
VENTURE [10]	Extrapolated	1.02959

Figure 5 shows the solution for the thermal flux distribution for the line $x=0$. Figure 6 shows the thermal flux deviation in percent for the three solutions with respect to the solution of the code MEDIUM-2 with a mesh size of 3 1/3 cm [6]: figure 6(a) is for the solution with 20 cm mesh and 3rd order expansion; (b) is for the 20 cm mesh and 5th order expansion; and, (c) is for the 10 cm and 3rd order.

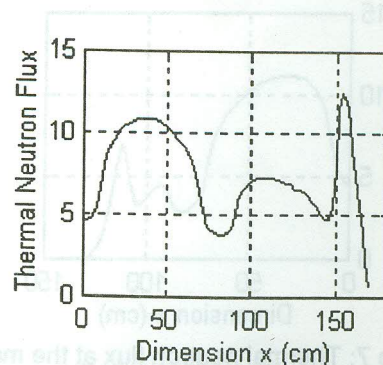


Figure 5: Thermal neutron flux at the line $x=0$.

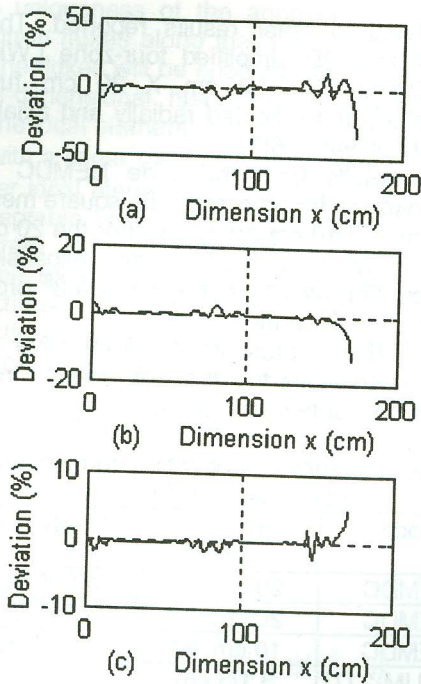


Figure 6: Relative deviation in percent of the thermal neutron flux at $x=0$, for the three solutions; (a) 20 cm, 3rd order; (b) 20 cm, 5th order; and, (c) 10cm, 3rd order.

Figure 7 shows the HEMDC solution for the thermal flux distribution for the main diagonal (line $y=x$). Figure 8 shows the thermal flux deviation in percent for the three solutions with respect to the results of the code MEDIUM-2 with a mesh size of 3 1/3 cm [6]: figure 8(a) is for the solution with 20 cm mesh and 3rd order expansion; (b) is for the 20 cm mesh and 5th order expansion; and, (c) is for the 10 cm and 3rd order.

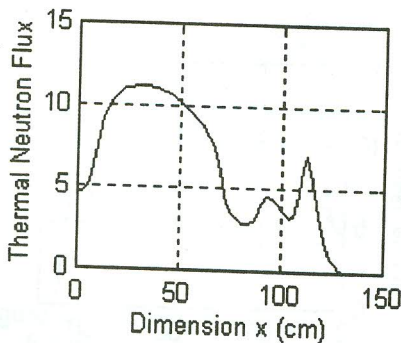


Figure 7: Thermal neutron flux at the main diagonal (line $y=x$)

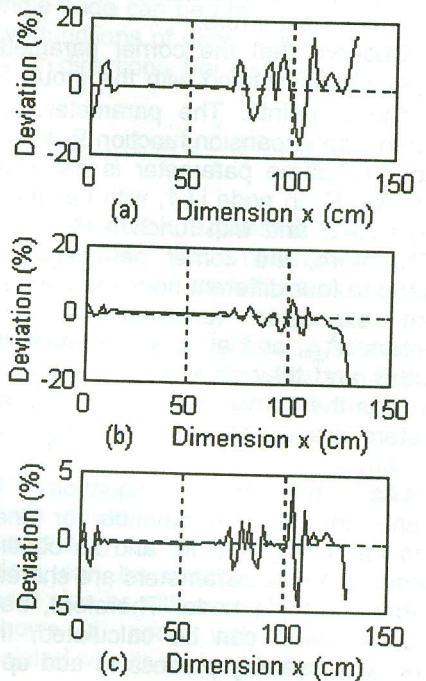


Figure 8: Relative deviation in percent of the thermal neutron flux at $y=x$, for the three solutions; (a) 20 cm, 3rd order; (b) 20 cm, 5th order; and, (c) 10cm, 3rd order.

Form figures 6 and 8 we observe that the relative deviation between the local fluxes calculated from the codes HEMDC and MEDIUM-2 are very small, less than 5% for the solution with a mesh of 10 cm and 3rd order expansion.

Table 2 shows the number of unknowns per group for the code HEMDC for the three cases.

Table 2: Number of unknowns per group for the three solutions of the code HEMDC

Case	Number of Unknowns
20cm, 3 rd	365
20 cm, 5 th	725
10 cm, 3 rd	1301

1/8th of the core.

The convergence criteria used is as follows,

$$\text{Max} \left| \frac{\bar{\Phi}_{g(i,j)}^t - \bar{\Phi}_{g(i,j)}^{t-1}}{\bar{\Phi}_{g(i,j)}^{t-1}} \right| < \epsilon$$

where $\bar{\phi}_{g(i,j)}^t$ is the average group flux for node i,j , and t is the t^{th} outer iteration. The numerical value used for ϵ was 10^{-5} .

The CPU time used for the code HEMDC is not compared with other codes in this work, because no attempt was made to develop a computational efficient code, only the method has been evaluated.

CONCLUSIONS

A nodal method for the solution of the two-dimensional two-group neutron diffusion equation in rectangular geometry has been developed and numerically evaluated. The method is based on the expansion of the group neutron fluxes by Legendre polynomials. The polynomials are adjusted in the rectangular nodes in a novel form, so that corner, side, and area functions are distinguished. The order of the approximation for the side and area expansion functions are up to desired or necessary degree. Numerical results for the two-dimensional IAEA benchmark problem have shown high accuracy for very coarse-mesh.

The simplicity of the method and the versatility of HEMDC enable the extension of the methodology to three-dimensional cases and to space-time diffusion applications, which are under development.

REFERENCES

- [1] Finnenmann, H., Bennewitz, F., and Wagner, M.R., "Interface Current Techniques for Multidimensional Reactor Calculation," Atomkernenergie, Vol. 30, pp. 123, 1977.
- [2] Langenbuch, W., Maurer, W., and Werner, W., "High Order Schemes for Neutron Kinetics Calculation, Based on Local Polynomial Approximation," Nucl. Sci. Eng., Vol. 64, pp. 508-516, 1977.
- [3] Chao, Y.A., and Penkrot, J.A., "Diffusive Homogeneity - The Principle of the Superfast Multi-Dimensional Nodal Code, SUPERNOVA," Trans. Am. Nucl. Soc., Vol. 55, pp. 583-584, 1987.
- [4] Nakata, H., and Martin, W. R., "The Finite Element Response Matrix Method," Nucl. Sci. Eng., Vol. 85, pp. 289-305, 1983.
- [5] Zienkiewicz, O.C., and Morgan, K., "Finite Elements and Approximation," John Wiley & Sons, New York, 1983.
- [6] "Benchmark Problem Book," ANL-7416 Suppl. II, Argonne National Laboratory, 1977.
- [7] Wagner, R. M. et al, "Validation of the Nodal Expansion Method and the Depletion Program MEDIUM-2 by Benchmark Calculations and Direct Comparison with Experiments," Atomkernenergie, Vol. 30, pp. 129, 1977.
- [8] Misfeldt, Ib, "Solution of the Multigroup Neutron Diffusion Equations by the Finite Element Method," Riso-M-1809, 1975.
- [9] Jatuff, F.E., and Gho, C.J., "A Response Matrix High-Order Nodal Method for Rectangular and Hexagonal Lattices," VIII Brazilian Meeting on Reactor Physics and Thermal Hydraulics, 17-20 Sept., Atibaia, 1991.
- [10] Vondy, D.R., Fowler, T.B., and Cunningham, G.W., "VENTURE: A Code Block for Solving Multigroup Neutronics Problems Applying the Finite-Difference Diffusion-Theory Approximation to Neutron Transport," Technical Report ORNL-5062, Oak Ridge National Laboratory, 1975.